17-(Allylamino)-17-demethoxygeldanamycin activity in human melanoma models

Angelika M. Burger[a], Heinz-Herbert Fiebig[a], Sherman F. Stinson[b] and Edward A. Sausville[b]

17-(Allylamino)-17-demethoxygeldanamycin (17-AAG) is a semisynthetic antitumor agent, which has entered phase I/II clinical trials. Melanoma cell lines in the NCI *in vitro* screen (mean GI_{50} = 84 nM) were relatively sensitive to the agent, which was therefore tested *in vivo* in four s.c. growing human melanoma xenografts (MEXF 276, 989, 462 and 514) in athymic mice. 17-AAG markedly inhibited tumor growth at doses of 80 (maximum tolerated dose) and 60 mg/kg/day in a qd × 5 (h: 0, 6; i.p.) schedule in two of four xenograft models. Cell lines derived from the 17-AAG-sensitive MEXF 276 and -resistant MEXF 514 melanomas, MEXF 276L and 514L, were chosen to study the effects of 17-AAG on its target Hsp90 as well as the Hsp90 'client' protein c-Raf-1 *in vitro*. Cells were exposed to drug concentrations which just cause total growth inhibition (total growth inhibition = 375 nM in MEXF 276L and 10 μM in MEXF 514L). Pharmacokinetic determinations confirmed that 17-AAG concentrations producing growth inhibition *in vitro* are readily achievable *in vivo* at the MTD ($AUC_{0-\infty}$ 1068 μM·min). Whilst 17-AAG treatment did not affect Hsp90 expression in the relatively resistant MEXF 514L cells, it caused a rapid transient decline in the markedly sensitive MEXF 276L cell line. In contrast, Hsp72 expression increased. Following Hsp90 depletion at 2–8 h in MEXF 276L cells, down-regulation of c-Raf-1 was seen starting at 16 h after drug addition. In MEXF 276 xenograft tissues treated with effective dose levels, loss of Hsp90 was seen and was associated with occurrence of apoptotic figures. The apoptotic index rose from 9% after 48 h, greater than 12% at 72 h to 45% at 10 days. These data support the hypothesis that in some melanoma models, a very good response (e.g. with tumor regressions) to 17-AAG may be associated with modulation of Hsp90 expression. The expression of this target should be followed in clinical studies with 17-AAG. *Anti-Cancer Drugs* 15:377–387 © 2004 Lippincott Williams & Wilkins.

Anti-Cancer Drugs 2004, **15**:377–387

Keywords: ansamycin, c-Raf-1, Hsp90, melanoma, cancer treatment

[a]Tumor Biology Center, Albert Ludwigs University of Freiburg, Freiburg, Germany and [b]Developmental Therapeutics Program, Division of Cancer Treatment and Diagnosis, National Cancer Institute, Bethesda, MD, USA.

Sponsorship: This work was funded in part by a contract from the NIH National Cancer Institute, Developmental Therapeutics Program to H. H. F. and the Deutsche Forschungsgemeinschaft/DFG with a grant to A. M. B.

Correspondence to E. A. Sausville, Office of the Associate Director, Developmental Therapeutics Program, NCI, EPN, Room 8018, 6130 Executive Boulevard, Rockville, MD 20852, USA.
Tel: +1 301 496-8720; fax: +1 301 402-0831;
e-mail: sausville@nih.gov

Received 5 September 2003 **Revised form accepted** 7 January 2004

Introduction

17-(Allylamino)-17-demethoxygeldanamycin (17-AAG, NSC 330507, Fig. 1) is a semisynthetic derivative of the naturally occurring anticancer agent geldanamycin (GA). Although GA itself has potent antiproliferative activities *in vitro*, its poor toxicologic and formulation features precluded its clinical development [1–3]. 17-AAG emerged from continued screening to identify GA analogs with a more favorable therapeutic index [4]. 17-AAG exhibits a differential cytotoxicity profile against several tumor types in the NCI 60 human tumor cell line panel including colon cancers and melanomas. The mean 50% growth inhibitory concentration (GI_{50}) over all cell lines is 150 nM; however, the melanoma subpanel is relatively more sensitive, with average melanoma GI_{50} = 84 nM in the 48-h sulforhodamine B (SRB) assay of the National Cancer Institute (NCI) *in vitro* screen [5]. Furthermore, pharmacologically active 17-AAG concentrations can be exceeded in mouse plasma or tissues and human tumor xenografts *in vivo* [6,7].

The heat shock protein Hsp90 has recently been identified as a molecular target for GAs [1,8]. The Hsp90 chaperone is required for the activation of several families of eukaryotic protein kinases and nuclear hormone receptors, many of which are proto-oncogenes such as c-Raf-1, c-ErbB2 and v-Src [1,8–11]. Moreover, Hsp90 seems to stabilize mutant p53, leading to accumulation of the latter in cancer cells, and is also necessary for the assembly of active telomerase from its catalytic subunit and RNA component [12,13]. The capacity to modulate the functions of these targets is the basis for interest in 17-AAG as a potential treatment modality for cancer. Proteins dependent upon Hsp90 for their proper folding or function are known as 'client proteins'. Many studies have identified cell growth inhibition *in vitro* and *in vivo* in model systems in response

0959-4973 © 2004 Lippincott Williams & Wilkins DOI: 10.1097/01.cad.0000124496.74538.e4

Fig. 1

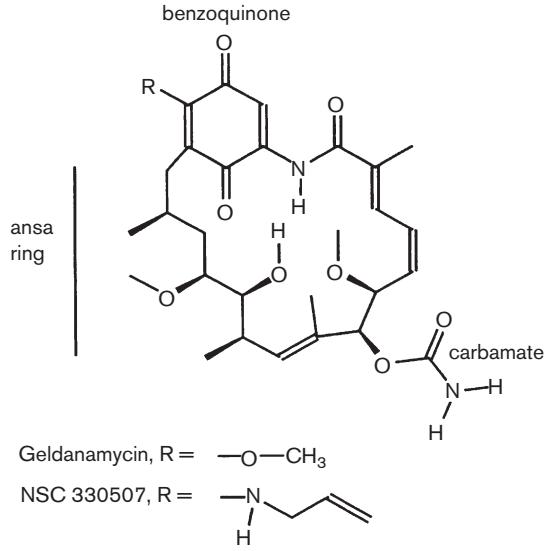

Molecular structure of 17-AAG.

to 17-AAG treatment and in association with modulation of client protein function. In view of the relative sensitivity of melanoma cells to 17-AAG, we wished to explore in an independently derived series of melanoma models whether 17-AAG action could be related to the function of its molecular target, Hsp90.

We examined the antiproliferative activity of 17-AAG in a panel of xenograft derived human melanoma cell lines *in vitro* and assessed whether 17-AAG's marked cytotoxicity found *in vitro* could be translated into efficacy *in vivo* in xenograft models. We correlated 17-AAG cytotoxicity with modulation of the Hsp90 chaperone molecule in a sensitive versus a resistant melanoma *in vitro* and *in vivo*. We report here that concentrations of drug found in mice at doses associated with preclinical activity are well within the range necessary from *in vitro* studies. In the highly responsive melanoma model, evidence of Hsp90 down-modulation preceded evidence of tumor cell apoptosis and regression. Our results point to the potential desirability of monitoring Hsp90 expression as well as key client proteins such as c-Raf-1 to correlate with response in clinical trials of 17-AAG.

Materials and methods

Drug

17-AAG, NSC 330507 (Fig. 1), was from the Pharmaceutical Resources Branch, NCI. For *in vivo* studies, the drug was prepared fresh daily in 10% dimethylsulfoxide (DMSO) and PBS containing 0.05% Tween 80 (PBS-T). First, the drug was dissolved in DMSO and then PBS-T was added to obtain the required final concentration in an injection volume of 10 ml/kg. The resulting formulation was a microfine suspension. *In vitro* experiments were performed with the drug dissolved in DMSO only and the working stock solution was 5 mM.

Cell lines and xenografts

Human tumor xenografts were established from freshly resected patient tumor material and kept in serial passage until stable growth. MEXF (melanoma xenograft Freiburg) 989, 462 and 276 are derived from lymph node or lung metastases of amelanotic melanomas; MEXF 514 is a melanotic melanoma derived from a lymph node metastasis [14]. An overview of tumor characteristics and that of cell lines derived thereof is given in Table 1.

The melanoma cell lines MEXF 276L, 514L and 462NL when injected into nude mice resemble the histology of the original xenograft and human primary from which they were derived [15]. A permanent cell line for MEXF 989 is not available. The tumor cell lines were grown at 37°C in a humidified atmosphere (5% CO_2) as monolayer cultures in RPMI 1640 medium supplemented with 10% FCS, 300 mg/l L-glutamine and gentamycin (50 µg/ml). Cells were trypsinized upon passage and maintained routinely. All cell lines were *Mycoplasma* free.

SRB assay

The 48-h SRB assay to assess the effect of drug on cell proliferation as measured by total cell protein was performed according to Skehan *et al.* [16]. Individual experiments were performed in replicates of eight wells/drug concentration and four independent experiments were carried out.

Clonogenic assay

Solid human melanoma xenografts growing s.c. in serial passages in nude mice (NMRI *nu/nu* strain) were removed under sterile conditions at a size of approximately 1 cm^3. Single-cell suspensions and soft agar cultures were prepared and drug added as described before [17,18]. Each drug concentration was added in triplicate wells and three or four independent experiments were performed. The TCA assay has the advantage that tumor material can be tested *in vitro* for selection of suitable *in vivo* models, even if no permanent cell line exists, as it is the case for MEXF 989 and other tumors of the Freiburg xenograft panel. On average, tumor stem cells, which are assayed in the TCA, are a log-fold more sensitive to drugs than a tumor cell line population [14,15].

Assessment of the *in vivo* activity of 17-AAG in human melanoma xenografts

All animal experiments were performed in accordance to the German animal protection act and project license regulations.The GA analog NSC 330507 was tested for *in vivo* antitumor activity in four human s.c. growing melanoma models MEXF 276, 989, 462 and 514. Athymic

Table 1

Tumor designation (human melanoma)	Histology/mets	Tumor doubling time (days)	PD of cell line (h)	No. of responses to standard agents *in vivo*	Response evaluation
MEXF 276	amelanotic (+) lymph node	3.0	33	0/13	resistant
MEXF 989	amelanotic (+) lung	5.2	NA	3/7	sensitive to DTIC, VCR, VIND
MEXF 462	amelanotic (+) peritoneum	1.5	28	4/5	sensitive to DTIC, IFO, VIND, taxol
MEXF 514	melanotic (+) lymph node	10.6	29	0/13	resistant

Standard agents tested: adriamycin, bleomycin, CCNU, cyclophosphamide, DTIC (dacarbazine), 5-FU, HECNU, ifosphamide (IFO), mitomycin C, methotrexate, mitoxantrone, cisplatin, tamoxifen, vinblastine, vincristine (VCR), vindesine (VIND), taxol, etoposide. Mets = derived from metastasis; NA, not analyzed because permanent cell line not available. PD = population doubling time of xenograft-derived cell lines under tissue culture conditions.

NCR nude mice, 6–8 weeks old, supplied by Charles River (Frederick, MD), were used for all experiments and tumors in passages 7–15 implanted s.c. as 3×4 mm fragments in both flanks. Animals were randomly assigned and treatment was initiated when tumors reached a volume of 100–120 mm^2. The control group received the DMSO/PBS-T vehicle formulation. An average group size of six animals ($n = 12$ tumors) was used to determine drug efficacy and at least two independent experiments were performed. Tumor growth was followed by serial caliper measurement and body weight documented concomitantly. Tumor volumes were calculated using the formula $(\text{length} \times \text{width}^2)/2$, where length is the largest dimension and width the smallest dimension perpendicular to the length. Relative tumor volumes were determined for each tumor by dividing the tumor volume on day X by the tumor volume on day 0 at the time of randomization. Tumor doubling time of test and control groups was defined as the period required to double the initial tumor volume (200%). A partial remission was defined as $T_X/T_0 = 10$–75% and a complete remission as $T_X/T_0 < 10\%$. Growth curves were analyzed in terms of maximal tumor inhibition [treated/control (T/C), calculated as median tumor weight of treated divided by median tumor weight of control animals $\times 100$] and growth delay (the difference in days to double the initial tumor volume of the test minus the control groups). Toxicity was assessed by lethality of tumor-bearing nude mice and body weight loss. At the maximum tolerable dose (MTD), the mice were allowed approximately a LD_{10} [19]. Statistical significance of drug effects was tested using the Mann–Whitney U-test.

Plasma pharmacokinetics of i.p. administered 17-AAG

A group of male, adult NCR *nu/nu* mice was given a single i.p. injection of 40 mg/kg body weight 17-AAG prepared as described above. Plasma was collected from three mice at each of eight scheduled intervals from 2 min through 6 h after administration. Another group of mice was treated in an identical manner, but received a second i.p. injection of 40 mg/kg 17-AAG after an interval of 6 h. From this group, plasma was collected from three mice at each of eight scheduled intervals from 5 min through 24 h after the second dose.

Plasma samples were analyzed by HPLC using the method of Supko *et al.* [2] with minor modifications. Briefly, samples (50 µl) were prepared for analysis by precipitation of plasma proteins with 150 µl of acetonitrile containing GA (0.7 µg/ml) as an internal standard (IS). The mixtures were vortexed vigorously for 1 min, centrifuged for 5 min at 13 000 g in a refrigerated centrifuge (4°C) and 165 µl of the supernatant was combined with 165 µl of 0.05 M ammonium acetate buffer (pH 4.7). A volume of 280 µl was injected on the column. The analytical system consisted of a 3.9×150 mm Waters Nova Pak C_{18} analytical column (Millipore, Milford, MA) coupled to a HP 1050 series quaternary pump and autosampler (Hewlett Packard, Palo Alto, CA). The column was maintained at ambient temperature and eluted isocratically at a flow rate of 1 ml/min with a mobile phase composed of methanol:0.05 M, pH 4.7, ammonium acetate buffer (67:33, v/v). The column effluent was concurrently monitored at wavelengths of 304 and 334 nm with a HP 1050 series UV diode array detector to detect the IS and 17-AAG, respectively. The analytical system was interfaced to a computer with HP software installed which was responsible for module control, and data acquisition and analysis. Calibration curves were constructed by plotting the ratio of the chromatographic peak areas of 17-AAG to the IS against the known analyte concentration in plasma standards. Twelve standards covering a concentration range from 0.02 (lower limit of quantitation) to 20 µM were employed. Linear least-squares regression analysis was performed to determine the slope and y-intercept of the best-fit line. Analyte concentrations in unknown samples were calculated by interpolation from the regression line. Each unknown sample was initially assayed in duplicate, with additional analyses performed if the replicate determinations deviated from their average by more than 10%. Samples with 17-AAG concentrations above the range of the standard curve were diluted with fresh mouse plasma and re-assayed. Plasma concentration–time profiles were constructed using the geometric mean of the plasma concentrations for the individual animals at each time point and the mean of the times of collection. The plasma concentration–time data was subjected to computer assisted, iterative, non-linear least-squares regression analysis

(Jandel Scientific, San Rafael, CA) and the pharmacokinetics was evaluated as previously described [20].

Immunohistochemistry

Treated MEXF 276 tumors were collected from mice receiving 80, 60, 40 and 20 mg/kg/day 17-AAG after 48, 56 and 72 h and on day 10, the time of maximum antitumor effect (tumor regression). Freshly removed tumor tissues were fixed in 4% PBS-buffered formalin for 24 h and then embedded in paraffin following standard procedures [21]. Tumors were cut in 4-μm sections, dried and then dewaxed. Endogenous peroxide was blocked by incubation in 3% H_2O_2 in methanol. Tissue sections were rehydrated in PBS (10 min) and exposed to 0.1% trypsin (Difco BD, Sparks, MD) in PBS (pH 7.8) for 20 min at 37°C. Unspecific binding sites were blocked by applying 10% normal goat serum in PBS for 30 min, then primary antibodies were added for 2 h (dilution 1:25) and negative control sections were treated with mouse IgG instead. The HistoStain SP kit (rabbit; Zymed, San Francisco, CA) based on a biotin–streptavidin/peroxidase/diaminobenzidine detection system was used for further processing. The sections were counter-stained with hematoxylin, dehydrated and mounted. Monoclonal mouse Hsp90 antibodies were from Transduction Laboratories (Lexington, KY); monoclonal mouse Hsp72 antibodies were from Oncogene Research Products (Bad Soden, Germany). Results were documented using a Zeiss light microscope (Jena, Germany) with an attached Kodak Digital Imaging System (Life Technologies, Karlsruhe, Germany).

Apoptosis index

The procedure described by Mukherjee *et al.*[22] was used to determine the number of apoptotic cells in 17-AAG-treated versus -untreated melanoma xenograft tissues. One hundred cells in three representative areas of three tumors per group were counted by use of a light microscope (Zeiss) at × 400 magnification. The apoptotic index (AI) was expressed as percentage AI (%) = $A \times 100/(A + C)$, where A = apoptotic cells and C = unaffected tumor cells.

Western blot analysis

Melanoma and normal mouse tissues were collected from untreated control mice. Cell lines were seeded in six-well plates (5×10^6 cells/5 ml/well) and allowed to attach overnight. Cells were exposed to concentrations of 17-AAG causing total growth inhibition for 0.5, 1, 2, 4, 8, 16, 24 and 48 h or 5 days, and harvested by scraping. Cell pellets or 50 mg tissues were washed with PBS and lysed in 100 μl of a (3-[(3-cholamidopropyl)dimethyl-ammonio]-1-propane-sulfonate) (CHAPS)-based lysis buffer (10 mM Tris–HCl, pH 7.5, 1 mM $MgCl_2$, 1 mM EGTA, 0.1 mM PMSF, 5 mM 2-mercaptoethanol, 0.5% CHAPS and 10% glycerol). Homogenates were kept on ice for 30 min and then centrifuged at 13 000 r.p.m. (Haereus, Hanau, Germany). The supernatants were collected and stored at –20°C. The protein content was determined using the Bio-Rad Protein Assay (Bio-Rad, Munich, Germany) [23]. Aliquots of 20 (Hsps) or 50 μg (c-Raf-1) of total cellular protein were loaded onto 4–12% Tris–glycine gradient gels (Novex, San Diego, CA) and separated using SDS–PAGE electrophoresis [24]. Following the transfer onto an ECL Hybond membrane (Amersham, Little Chalfont, UK), blots were processed using an ECL Chemiluminescence Western blotting kit (Amersham). Monoclonal mouse antibodies (mmAb) for Hsp90 and c-Raf-1 were from Transduction Laboratories (Lexington, KY), mmAb Hsp72/73 was from Oncogene Research Products (Bad Soden, Germany) and mmAb pan-actin from Dianova (Hamburg, Germany). Actin antibodies were used as controls to ensure equal gel loading. In addition, polyacrylamide gels were stained with Coomassie blue after the transfer procedure.

Results

In vitro antiproliferative activity

Prior studies of 17-AAG have shown that this agent is a potent inhibitor of human tumor cell growth. With an average GI_{50} in the NCI *in vitro* cancer drug screen of 150 nM, six of eight melanoma cell lines were clearly more sensitive than average, with a mean GI_{50} of 84 nM [5]. Potential selectivity for melanoma was independently confirmed in the Freiburg screening panel, which included the human melanoma xenografts MEXF 276, 989, 462 and 541, and cell lines derived from them (MEXF 276L, 514L and 462NL) (Table 1 and Fig. 2). In Figure 2, 17-AAG activity was tested against melanoma cells derived from xenografts, but grown *in vitro* using the clonogenic assay (TCA; Fig. 2B), and in permanent melanoma cell lines growing in 96-well plates by the SRB method (Fig. 2A). 17-AAG was most active *in vitro* in both MEXF 276 systems with $GI_{50} < 0.02$ nM in the clonogenic assay and $GI_{50} = 70 \pm 8$ nM in the SRB (Fig. 2A and B). MEXF 989 ($GI_{50} = 2$ nM in the TCA), MEXF 514 ($GI_{50} = 4$ nM, TCA; 125 ± 11 nM SRB) and MEXF 462 ($GI_{50} = 410$ nM, TCA; 250 ± 23 nM SRB) were less sensitive.

17-AAG was markedly more active in the 5- to 15-day soft agar assay when compared to the 48-h SRB, suggesting that tumor stem cells and anchorage-independent growing cells may be more susceptible to 17-AAG (Fig. 2A and B). However, MEXF 276 and 276L, respectively, remained the most responsive xenograft and cell line, being over 100-fold more sensitive to 17-AAG at the GI_{50} level compared to MEXF 989, 462 and 514 *in vitro* (Fig. 2B). Differential MEXF 276 *in vitro* activity appears not to be related to population doubling time (PD) in culture (Table 1) since its PD of 33 h was similar to that of MEXF 514L (29 h) or 462NL (28 h).

Fig. 2

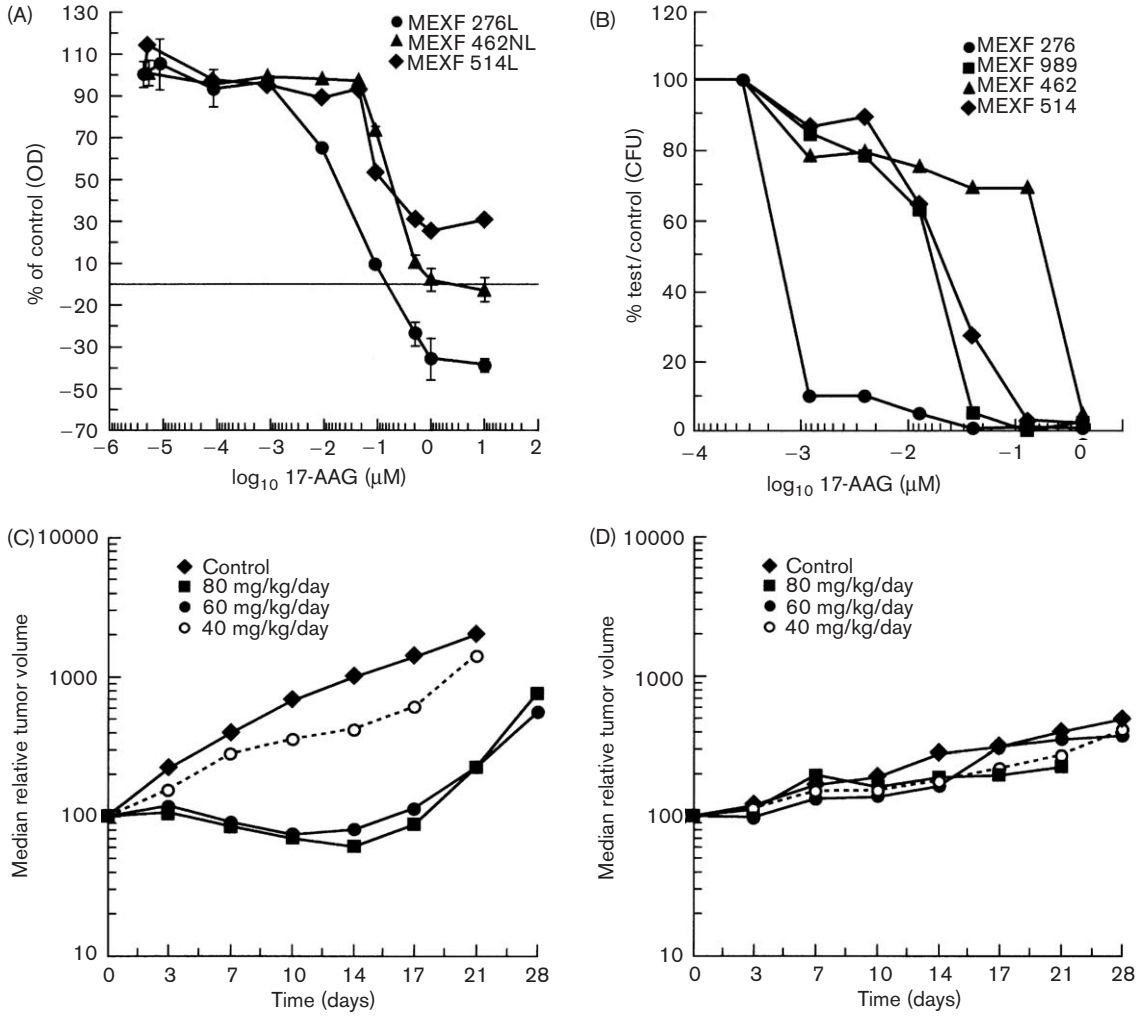

Effects of 17-AAG in human melanoma xenografts *in vitro* and *in vivo*. (A) Activity of 17-AAG in three melanoma xenograft-derived monolayer cell lines using the 48-h SRB assay procedure according to Skehan *et al.* [16]. Data are shown as percentage of control optical density at 550 nm: 100% MEXF 276L = 0.6, MEXF 462NL = 1.7 and MEXF 514L = 0.65 (ODs are corrected for non-specific background). Each data point represents the mean of four independent experiments. Negative numbers (*y*-axis) indicate that net cell kill occurred at termination of the assay compared to starting cell number (set as 0% growth). The TGI values for MEXF 276L = 375 ± 130 nM, MEXF 462NL = 6.700 ± 444 nM and MEXF 514L = 10.000 ± 250. (B) Activity of 17-AAG in four melanoma xenograft-derived cells in a clonogenic assay *in vitro*. Single-cell suspensions of enzyme-digested xenograft tissues were seeded into soft agar and their clonogenic potential followed under 17-AAG treatment. MEXF 276 was the most sensitive tumor with GI_{50}s around 0.02 nM; MEXF 989 (2 nM), MEXF 514 (4 nM) and MEXF 462 (700 nM) were much less responsive. Data are presented as T/C in percent of colony forming units (CFU). 100% MEXF 276 = 145 CFU, MEXF 514 = 89 CFU, MEXF 462 = 176 CFU and MEXF 989 = 191 CFU. CFU, mean of $n = 3$, SD = max ± 10%. (C) Antitumor activity of 17-AAG in the MEXF 276 xenograft model system, showing marked reduction of tumor growth with evidence of a significant tumor remission at 60 and 80 mg/kg/day. (D) Antitumor activity of 17-AAG in the MEXF 514 xenograft model system, which, in contrast to MEXF 276, did not respond *in vivo* to 17-AAG therapy.

In vivo activity of 17-AAG in human melanoma xenografts

17-AAG was evaluated for antitumor activity in four human melanoma xenografts in athymic nude mice (Table 2, and Fig. 2C and D). 17-AAG was highly active in the amelanotic, relatively chemoresistant melanoma MEXF 276 and the relatively chemosensitive amelanotic melanoma MEXF 989. Partial tumor remissions were seen (MEXF 276, 80 mg/kg/day: opt. T/C = 6%, 60 mg/kg/day: opt. T/C = 8%; MEXF 989 80 mg/kg/day: opt. T/C = 12%, 60 mg/kg/day: opt T/C = 19%) at doses of 80 and 60 mg/kg/day administered i.p. on days 1–5 and 8–12. In this active schedule, the daily dose was split, resulting into two injections given at 0 and 6 h; 80 mg/kg/day was found to be the MTD. If the drug was given to MEXF 276 tumor-bearing mice at 60 mg/kg/day as split doses on days 1–4, the antitumor effect of 17-AAG was considerably less pronounced and tumor growth inhibition was observed with an opt. T/C = 30.7% (day 10) only. A single daily injection was tolerated up to a dose of 45 mg/kg/day

Table 2 Activity of 17-AAG (NSC 330507) in melanoma xenografts

Melanoma model	Schedule	Drug dose (i.p. mg/kg/day)	Opt. T/C activity (days)	Growth delay (days)	Max. BWC (%)	Drug-related deaths (*n*/total)	Statistical significance
MEXF 276	1–5, 8–12 (h: 0, 6)	80 (MTD)	6.1 (14) + + +	18.0	+6.3	1/8	$p<0.001$
MEXF 276	1–5, 8–12 (h: 0, 6)	60	8.0 (17) + +	17.8	+2.4	0/7	$p<0.001$
MEXF 276	1–5, 8–12 (h: 0, 6)	40	41.2 (14) +	2.1	+5.2	0/7	$p<0.05$
MEXF 276	1–4 (h: 0, 6)	60	30.7 (10) +	5.9	+13.5	0/6	$p<0.005$
MEXF 989	1–5, 8–12 (h: 0, 6)	80 (MTD)	12.6 (10) + + +	13.9	−21.1	1/5	$p<0.001$
MEXF 989	1–5, 8–12 (h: 0, 6)	60	18.7 (10) + + +	12.6	−14.4	1/5	$P<0.001$
MEXF 989	1–5, 8–12 (h: 0, 6)	40	81.4 (10)	−0.9	−9.0	0/5	NS
MEXF 989	1–5, 8–12	36	66.3 (28)	−1.1	−2.1	1/5	NS
MEXF 462	1–5, 8 (h: 0, 6)	80 (MTD)	59.1 (7)	−0.2	−1.4	1/6	NS
MEXF 462	1–5, 8 (h: 0, 6)	60	76.6 (4)	−0.4	−7.4	0/6	NS
MEXF 462	1–5, 8 (h: 0, 6)	40	90.5 (2)	−0.3	−9.8	0/5	NS
MEXF 514	1–5, 8–12 (h: 0, 6)	80 (MTD)	56.8 (21)	−6.1	−16.5	3/6	NS
MEXF 514	1–5, 8–12 (h: 0, 6)	60	58.5 (14)	−4.3	−4.7	2/6	NS
MEXF 514	1–5, 8–12 (h: 0, 6)	40	66.2 (14)	−5.8	+4.8	0/6	NS
MEXF 514	1–5, 8–12	45 (MTD)	82.2 (11)	−3.0	+8.5	0/5	NS

T/C>50%= (–); T/C>25–50%=(+); T/C<25%=(+ +); (+ + +)=partial remission; NS=not significant according to Mann–Whitney–Wilcoxon *U*-test. h: 0, 6=the total indicated drug dose was split in half and given at 0 and 6 h. Max. BWC=median maximal body weight change relative to starting weight at day of randomization in percent. Opt. T/C (day)=optimal T/C (day after randomization). (*n*/total)=number of drug-related deaths per total number animals in the group.

Fig. 3

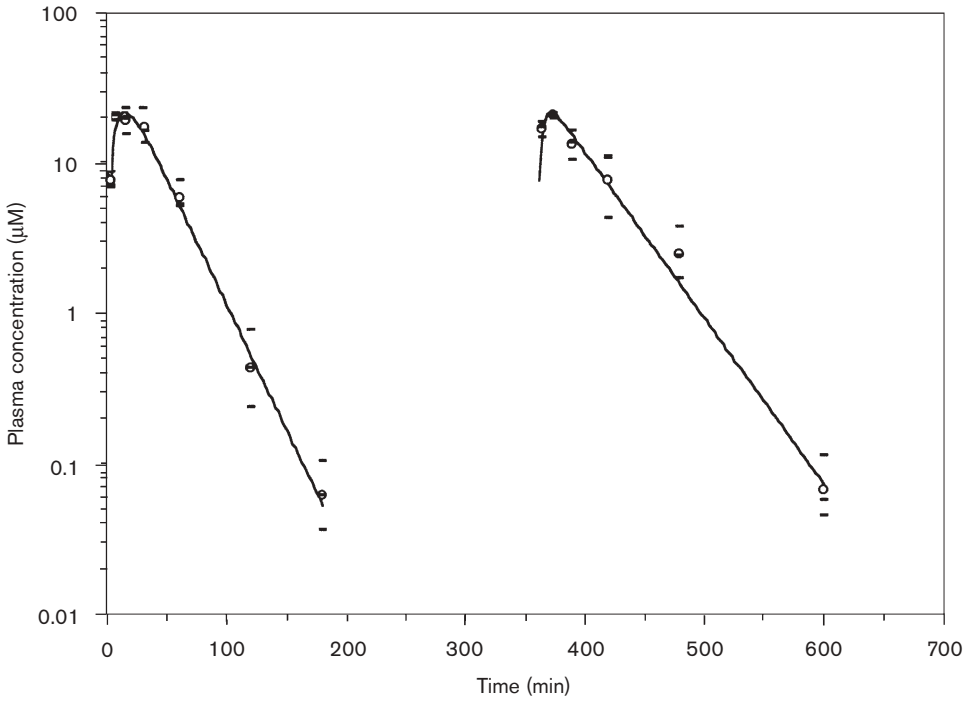

Mouse plasma pharmacokinetics of 17-AAG (80 mg/kg/day). Plasma concentrations and the line of best fit determined by non-linear regression analysis of data obtained following sequential i.p. administration of 40 mg/kg 17-AAG to NCR *nu/nu* mice at an interval of 360 min. Circles are the geometric mean concentrations and horizontal bars the individual animal data points.

(MTD single dose), but no noteworthy antitumor effect was seen.

The chemoresistant melanoma MEXF 514 and the fast growing MEXF 462 tumor were less sensitive towards GA analog treatment and did not respond with significant growth inhibition. However, the split dose of 80 mg/kg/day (MTD) was also more effective than the once daily administration of 45 mg/kg/day (single dose MTD) 17-AAG in these tumors (Table 2).

In summary, while partial tumor regressions seen in the MEXF 276 and 989 models with optimal T/Cs at 80 and 60 mg/kg/day between 6 and 8% (Fig. 2C) or 13 and 19% (Table 2), respectively, were highly significant ($p < 0.001$), no statistically significant effects were found

in MEXF 462 and 514 melanomas ($p > 0.05$, Fig. 2D and Table 2).

17-AAG Plasma levels at MTD

The plasma concentration–time profiles and lines of best fit determined by non-linear regression analysis of data obtained following i.p. administration of sequential 17-AAG doses at a 6-h interval of 40 mg/kg body weight to mice is shown in Figure 3. Plasma concentrations of 17-AAG increased rapidly, reaching peak levels of approximately 20 μM between 5 and 10 min after i.p. injection. Levels remained in the 5–10 μM range for 30–60 min and then decreased with a half-lives of 18.1 and 27.2 min after one or two sequential doses, respectively. Thus, plasma concentrations of 17-AAG were in excess of those producing total growth inhibition in *in vitro* assays for at least 2–3 h following each i.p. administration of 40 mg/kg. 17-AAG, however, was not detected in plasma samples collected later than 3–4 h after administration. The $AUC_{0-\infty}$ was 1068 μM·min after the first dose of 17-AAG and 1301 μM·min after the second. The bioavailabilities after the first and second i.p. doses were 97 and 119%, respectively.

Hsp90 and c-Raf-1 expression in 17-AAG-sensitive and -resistant melanoma cell lines

Melanoma cell lines were treated for 0.5 h. to 5 days with drug concentrations which just cause total growth inhibition (375 nM for MEXF 276L and 10 μM in MEXF 514L cells). While 17-AAG did not affect Hsp90 expression in MEXF 514L (Fig. 4C), it caused a pronounced rapid, transient decline (2–8 h) in Hsp90 levels in the 17-AAG-responsive/sensitive MEXF 276L cells as shown by Western blot (Fig. 4A). In MEXF 276L cells, the decline correlated with 17-AAG-induced loss of Hsp90 by immunoperoxidase staining in *in vitro* cultured cells (data not shown). In contrast, Hsp72 expression was rather transiently increased at 24 and 48 h after 17-AAG exposure (Fig. 4A) in MEXF 276L cells.

Correlating with Hsp90 depletion, and thus loss of molecular chaperone function between 2 and 8 h at TGI concentrations of 17-AAG in sensitive MEXF 276L cells, down-regulation of effector proto-oncogenes and oncogenes such as c-Raf-1 was seen starting between 4 and 8 h after 17-AAG was added (Fig. 4B), and was markedly depleted under continuous exposure to 17-AAG at 16 and 24 s as the likely consequence of lack of Hsp90-mediated maturation/refolding and thus degradation of the abnormal Raf protein in the proteosome. In the 17-AAG-resistant MEXF 514L melanoma cell line, treatment with TGI concentrations had neither effect on Hsp90 levels nor on c-Raf-1 protein expression (Fig. 4C).

Fig. 4

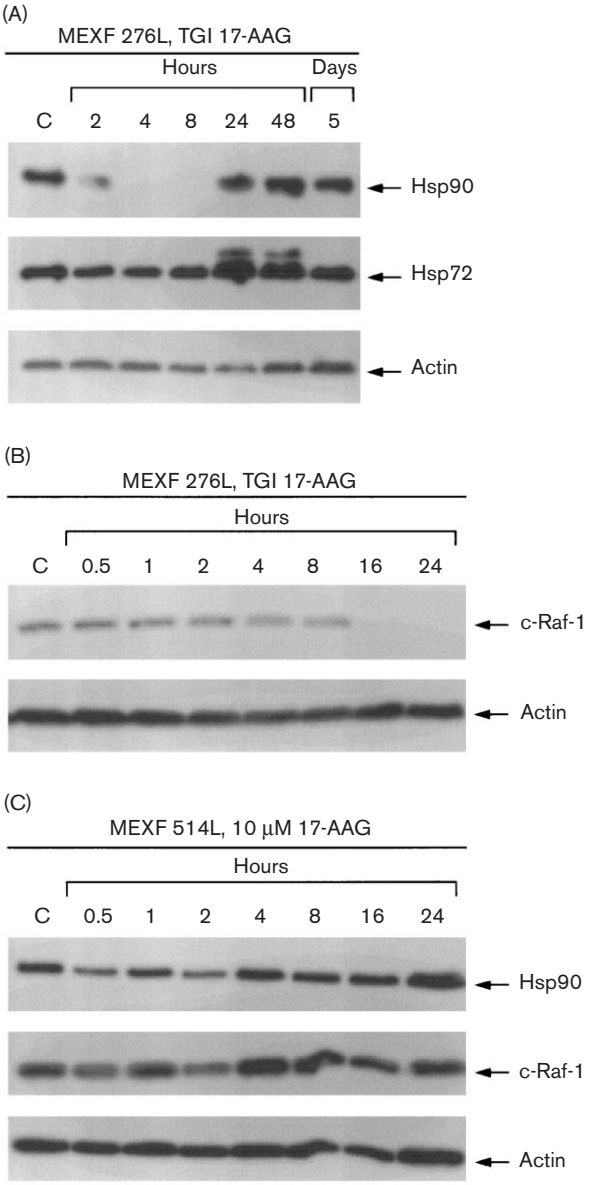

Depletion of Hsp90 and c-Raf-1 in the 17-AAG-responsive melanoma cell line MEXF 276L. (A) MEXF 276 L cells were exposed to 375 nM 17-AAG for 2, 4, 8, 24 and 48 h or 5 days and the expression of Hsp90, Hsp72 and pan-actin detected by Western blot. A band occurring above the specific 72-kDa signal for Hsp72 is non-specific. (B) MEXF-276L exposed to TGI concentrations for 0.5, 1, 2, 4, 8, 16 and 24 h, and then probed for c-Raf-1. (C) MEXF 514L, resistant to 17-AAG, shows no loss of Hsp90 nor effects on c-Raf-1 despite exposure to 17-AAG at the TGI concentration of 10 μM. Pan-actin was used as equal loading control.

Hsp90 modulation induces apoptosis in 17-AAG-responsive tumors *in vivo*

The modulation of Hsp90 expression which was seen in the 17-AAG-responsive, xenograft-derived cell line MEXF 276L, but not in the resistant MEXF 514L cell line (Fig. 4), was also observed in xenograft tumors *in vivo*

Fig. 5

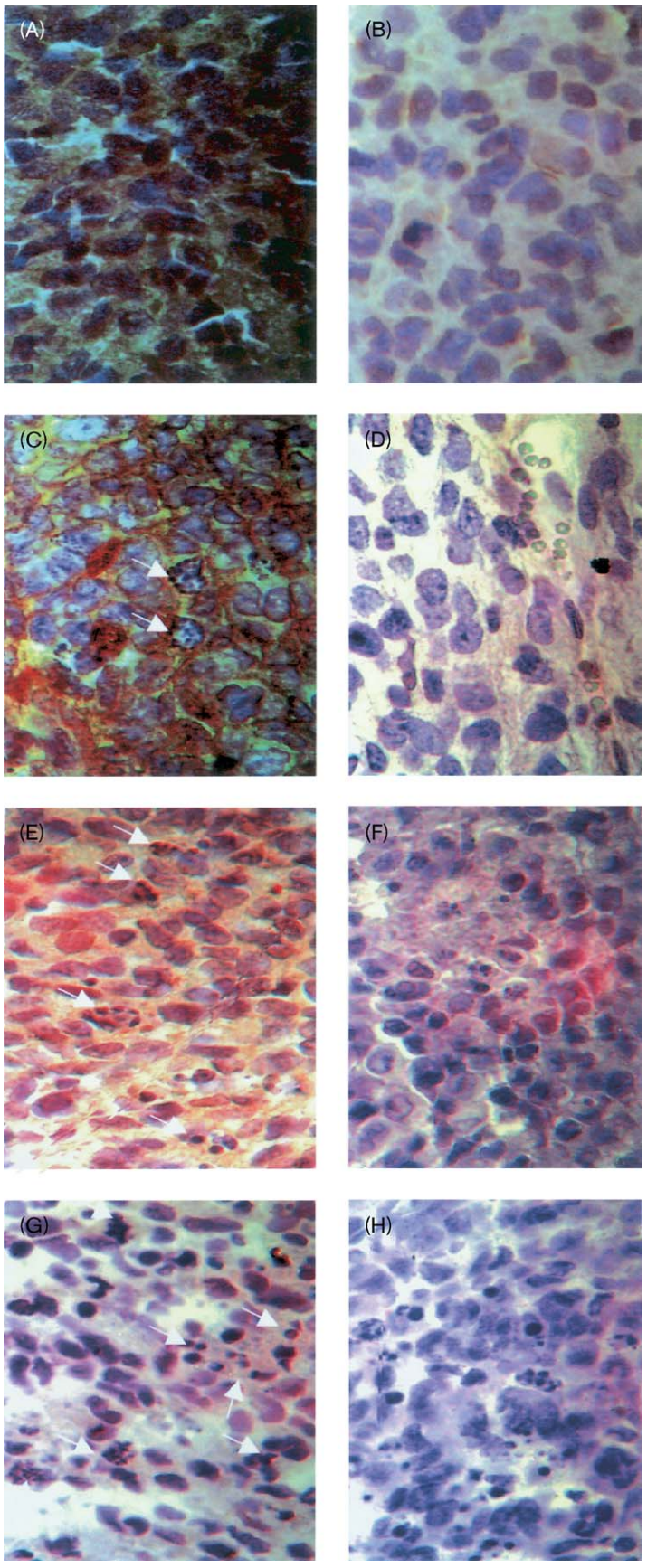

Depletion of Hsp90 is associated with the appearance of apoptotic figures in the 17-AAG-treated MEXF 276 xenograft. Shown are anti-Hsp90-probed MEXF 276 tissues (a, c, e and g) and their hematoxylin-stained counterparts, which were only incubated with non-specific immunoglobulins (=negative controls, b, d, f and h). Hsp90 expression appears as a brown diaminobenzidine/peroxidase product. A gradual decrease of Hsp90 concomitant with an increase in apoptosis occurs compared to control MEXF 276 samples (a and b) in tumors removed at 48 h (c and d) 72 h (e and f) and 10 days (g and h) under effective dose 17-AAG treatment (here, 80 mg/kg/day, i.p., qd $\times$ 5, h: 0, 6, over 2 weeks). The arrows indicate apoptotic bodies observed after 17-AAG treatment. Magnification $\times$ 600.

(Fig. 5). Hsp90 levels decreased with time and a complete lack of Hsp90 expression was seen in MEXF 276 specimens treated with effective 17-AAG doses at the time of maximum antitumor effect (partial remission). The effects on Hsp90 expression, however, were dependent on the 17-AAG dose administered. At the merely equieffective doses of 80 and 60 mg/kg/day with optimal T/Cs of 6.1 and 8%, respectively (see Table 2), Hsp90 levels diminished over time as shown in Fig. 5(a, c, e and g) for 80 mg/kg/day. In contrast, at marginally or ineffective 17-AAG concentrations such as 40 (Table 2) or 20 mg/kg/day, changes in Hsp90 expression could not be observed (data not shown). Moreover, similar results were found when MEXF 989 tissue obtained from control and 80-mg/kg/day animals at maximum 17-AAG effect was stained for Hsp90, confirming that responsiveness to 17-AAG is related to modulation of Hsp90 protein levels (data not shown). In 80- mg/kg/day 17-AAG-treated MEXF 276 tumors, loss of Hsp90 was associated with subsequent marked occurrence of apoptotic figures (e.g. Fig. 5c, e and g). The apoptotic index rose from essentially 0% in control tumors to $9.3 \pm 0.9\%$ after 48 h of 17-AAG treatment and reached $12.6 \pm 1.2\%$ at 72 h. At 10 days after 17-AAG treatment was initiated, the apoptotic index went up to $45.6 \pm 5.2\%$ accompanied by tumor shrinkage (Figs 5g and 2C). At no effect level doses, e.g. 40 and 20 mg/kg/day, apoptosis was not seen (data not shown).

Discussion

We have shown here that 17-AAG is a potently active cytotoxic agent *in vitro* and shows marked antitumor activity at tolerated doses in melanoma xenografts *in vivo*. It was highly active in the amelanotic melanoma MEXF 276 (resistant to standard chemotherapy) and the amelanotic melanoma MEXF 989. Partial tumor remissions were seen [MEXF 276: opt. T/C = 8 and 6% (day 14); MEXF 989: opt. T/C = 19 and 12% (day 10)] at doses of 60 and 80 mg/kg/day, respectively. We report here that doses and schedules of 17-AAG associated with evidence of tumor regressions are associated with down-regulation of Hsp90 along with subsequent effects on chaperone proteins such as in this case c-Raf-1.

A key question in the development of 'targeted' therapies is whether beneficial clinical effects of a drug can be associated with action on its molecular target. While numerous prior reports have documented effects of 17-AAG on c-ErbB2 [9], c-Raf-1 [10], Alk [25], Bcr–Abl [26], Akt [27] and estrogen receptor [28], the effect of the drug on the expression or function of its binding partner Hsp90 has not been consistently defined. We report here that the MEXF 276 melanoma model does display an effect of 17-AAG on Hsp90 levels as well as function, at doses and schedules associated with pronounced evidence of tumor regression.

Since Hsp90 is a highly prevalent cellular protein, these results raise the possibility that different client proteins will be differentially susceptible to modulation by 17-AAG depending on the extent to which Hsp90 may be 'titrated' by either the drug itself or drug acting in context with endogenous cellular determinants of Hsp90 turnover. This mechanism of drug effect would potentially exist in addition to the well-accepted model where Hsp90 is blocked from associating with improperly folded client proteins, which are then degraded. Thus, very susceptible tumors might have facile depletion of Hsp90 or a unique dependence on continued signaling from a protein such as c-ErbB2, which is readily displaced from Hsp90 and then degraded. We believe, therefore, that future studies of 17-AAG or other modulators of Hsp90 function might usefully address effects on Hsp90 levels as well as Hsp90-associated chaperoned molecules in correlating with tumor response.

By binding and inhibiting Hsp90, 17-AAG treatment has been shown to shift the binding of client proteins such as Bcr–Abl in K562 cells from Hsp90 to Hsp70 and this induces their proteasomal degradation [26]. The fact that we see an induction of Hsp72, the inducible form of Hsp70, upon loss of Hsp90 expression in the MEXF 276L melanoma cell line (Fig. 4A), is concordant with that observation. Hsp70 expression in mononuclear cells has been examined as surrogate marker for clinical trials and should be considered in concert with measurements of Hsp90 protein levels.

Plasma pharmacokinetics of 17-AAG at the MTD doses employed in this study (80 mg/kg/day i.p. split into two doses at 0 and 6 h) revealed that the drug is rapidly and efficiently absorbed following i.p. administration. Importantly, plasma concentrations of 17-AAG were in excess of those producing total growth inhibition and target effects in *in vitro* assays in the sensitive melanoma cell line MEXF 276L for at least 2–3 h after each injection. In view of the rapid, transient decrease (2–8 h) of Hsp90 protein in cultured MEXF 276L cells after exposure to 17-AAG (Fig. 4A), the period of 2–3 h in which TGI concentrations can be achieved in plasma, should be sufficient to establish 17-AAG effects. Eiseman *et al.* had found similar results in that they achieved drug levels in the order of TGI concentrations in mice bearing mammary carcinoma xenografts [6,7]. In addition, they found that tumor c-Raf-1 as well as Hsp90 were lower than that of the vehicle controls, and that c-Raf-1 and Hsps were less affected in liver, lungs, kidneys and spleens of the treated animals as compared to tumors, suggesting the possible prospect of favorable therapeutic index in Hsp90 modulation.

In agreement with this, by using immunohistochemistry and Western blot we have observed that Hsp90 levels of 17-AAG-sensitive tumors were much lower than those

of resistant xenograft models, and that mouse liver and lung Hsp90 protein expression was minimal (data not shown), indicating a lesser demand for Hsp90 chaperoning and a lesser degree of Hsp90 dependency in these tissues. Recent findings that a 100-fold increase of 17-AAG binding affinity in tumor versus normal tissue Hsp90 exists might also explain its tolerance by normal tissues and contribute to its therapeutic window [29].

Preliminary clinical phase I trial results for 17-AAG obtained in three different centers reflect our and the preclinical data of Eiseman *et al.* [6,7]. Measured peak drug levels below doses causing dose-limiting toxicity were well above *in vitro* effective drug concentrations, and there is initial evidence of Hsp90 client protein modulation in peripheral blood mononuclear cells [30–32] and tumor cells [33] from treated patients.

In conclusion, our data suggest that the efficacy of 17-AAG treatment in the highly responsive human melanoma xenograft model reported here is temporally correlated not only with the frequently described modulation of the c-Raf-1 proto-oncogene, but also with diminished levels of Hsp90, the molecular target of the drug itself. Prospective evaluation of Hsp90 levels, along with Hsp70- and Hsp90-associated chaperoned molecules might be considered in future clinical trials with these agents, particularly since initial suggestion of prolonged stabilization of certain melanoma patients in clinical trials has been described with 17-AAG [33].

Acknowledgments

We thank Victoria Smith, Kim Hill, Chris Bramhall, Elke Tetling and Julia Schüler for their excellent technical support.

References

1 Neckers L, Schulte TW, Mimnaugh E. Geldanamycin as a potential anti-cancer agent: its molecular target and biochemical activity. *Invest New Drugs* 1999; **17**:361–373.
2 Supko JG, Hichman RL, Frever MR, Malspeis L. Preclinical pharmacologic evaluation of geldanamycin as an antitumor agent. *Cancer Chemother Pharmacol* 1995; **36**:305–315.
3 Page J, Heath J, Fulton R, Yalkowsky E, Tabibi E, Tomaszewski J, *et al.* Comparison of geldanamycin (NSC-122750) and 17-allylaminogeldanamycin (NSC-330507D) toxicity in rats. *Proc Am Ass Cancer Res* 1997; **38**:308.
4 Schnur RC, Corman ML, Gallachun RJ, Cooper BA, Dee MF, Coty JL, *et al.* erbB-2 oncogene inhibition by geldanamycin derivatives: synthesis, mechanism of action, and structure–activity relationships. *J Med Chem* 1995; **38**:3813–3820.
5 Developmental Therapeutics Program Website: http://dtp.nci.nih.gov/, mean graph for compound S330507.
6 Eiseman JL, Sentz DL, Zuhowski EG, Ramsland TS, Rosen DM, Reyna SP, *et al.* Plasma pharmacokinetics and tissue distribution of 17-allylaminogeldanamycin (NSC 330507), a prodrug for geldanamycin, in CD2F1 mice and Fischer 344 rats. *Proc Am Ass Cancer Res* 1997; **38**:308.
7 Eiseman J, Grimm A, Sentz D, Lessor T, Gessner R, Zuhowski E, *et al.* A. Pharmacokinetics of 17-allylamino(17-demethoxy)geldanamycin in SCID mice bearing MDA-MB-453 xenografts and alterations in the expression of p185erb-B2 in the xenografts following treatment. *Clin Cancer Res* 1999; **5**:3837s.
8 Stebbins CE, Russo AA, Schneider C, Rosen N, Hartl FU, Pavletich NP. Crystal structure of an Hsp90–geldanamycin complex: targeting of a protein chaperone by an antitumor agent. *Cell* 1997; **89**:239–250.
9 Hartmann F, Horak EM, Cho C, Lupu R, Bolen JB, Stetler-Stevenson MA, *et al.* Effects of the tyrosine-kinase inhibitor geldanamycin on ligand-induced her-2/*neu* activation, receptor expression and proliferation of her-2-positive malignant cells. *Int J Cancer* 1997; **70**:221–229.
10 Schulte TW, Blagosklonny MV, Ingui C, Neckers L. Disruption of the Raf-1-Hsp90 molecular complex results in destabilization of Raf-1 and loss of Raf-1-Ras association. *J Biol Chem* 1995; **270**:24585–24588.
11 Whitesell L, Mimnaugh EG, DeCosta B, Myers C, Neckers LM. Inhibition of heat shock protein Hsp90–pp60$^{v\text{-}src}$ heteroprotein complex formation by benzoquinone ansamycins: essential role for stress proteins in oncogenic transformation. *Proc Natl Acad Sci USA* 1994; **91**:8324–8328.
12 Whitesell L, Sutphin PD, Pulcini EJ, Martinex JD, Cook PH. The physical association of multiple molecular chaperone proteins with mutant p53 is altered by geldanamycin, an hsp90-binding agent. *Mol Cell Biol* 1998; **18**:1517–1524.
13 Holt SE, Aisner DL, Baur J, Tesmer VM, Dy M, Quellette M, *et al.* Functional requirement of p23 and Hsp90 in telomerase complexes. *Genes Dev* 1999; **13**:817–826.
14 Fiebig HH, Berger DP, Dengler WA, Wallbrecher E, Winterhalter BR. Combined *in vitro*/*in vivo* test procedure with human tumor xenografts. In: Fiebig HH, Berger DP (editors): *Immunodeficient Mice in Oncology*. Basel: Karger; 1992, pp. 321–351.
15 Roth T, Burger AM, Dengler W, Fiebig HH, Monks A, McMahon J, *et al.* Human tumor cell lines demonstrating the characteristics of patient tumors as useful models for anticancer drug development. In: Fiebig HH, Burger AM (editors): *Relevance of Tumor Models for Anticancer Drug Development*. Basel: Karger; 1999, pp. 145–156.
16 Skehan P, Storeng R, Scudiero D, Monks A, McMahon J, Vistica D, *et al.* New colorimetric cytotoxicity assay for anti-cancer drug screening. *J Natl Cancer Inst* 1990; **82**:1107–1112.
17 Hamburger AW, Salmon SE. Primary bioassay of human tumor stem cells. *Science* 1977; **197**:461–463.
18 Phillips RM, Burger AM, Jarrett C, Loadman PM, Fiebig HH. Predicting tumor responses to mitomycin C on the basis of DT-diaphorase activity or drug metabolism by tumor homogenates: implications for enzyme directed bioreductive drug development. *Cancer Res* 2000; **60**:6384–6390.
19 Burger AM, Hartung G, Stehle G, Sinn H, Fiebig HH. Preclinical evaluation of a methotrexate–albumine-conjugate (MTX–HSA) in human tumor xenografts *in vivo*. *Int J Cancer* 2001; **92**:718–24.
20 Stinson SF, House T, Bramhall C, Saavedra JE, Keefer LK, Nims RW. Plasma pharmacokinetics of a liver-selective nitric oxide-donating diazeniumdiolate in the male C57BL/6 mouse. *Xenobiotica* 2002; **32**:339–347
21 Burck CH. *Histologische Technik*. Stuttgart: Thieme; 1988.
22 Mukherjee P, Sotnikov V, Mangian HJ, Zhou J-R, Visek WJ, Clinton SK. Energy intake and prostate tumor growth, angiogenesis, and vascular endothelial growth factor expression. *J Natl Cancer Inst*, 1999; **91**: 512–523.
23 Bradford MM. A rapid and sensitive method for the quantification of microgram quantities of protein utilizing the principle of protein-dye binding. *Anal Biochem* 1976; **72**:248–254.
24 Laemmli UK. Cleavage of structural proteins during the assembly of the head of bacteriophage T4. *Nature* 1970; **227**:680–685.
25 Bonvini P, Gastaldi T, Falini B, Rosolen A. Nucleophosmin-anaplastic lymphoma kinase (NPM-ALK), a novel Hsp90-client tyrosine kinase: down-regulation of NPM-ALK expression and tyrosine phosphorylation in ALK$^+$ CD30$^+$ lymphoma cells by the Hsp90 antagonist 17-allylamino,17-demethoxygeldanamycin. *Cancer Res* 2002; **62**:1559–1566.
26 Nimmanapalli R, O'Bryan E, Bhalla K. Geldanamycin and its analogue 17-allylamino-17 demethoxygeldanamycin lowers Bcr–Abl levels and induces apoptosis and differentiation of Bcr–Abl-positive human leukemic blasts. *Cancer Res* 2001; **61**:1799–1804.
27 Solit DB, Basso AD, Olshen AB, Scher HI, Rosen N. Inhibition of heat shock protein 90 function down-regulates Akt kinase and sensitizes tumors to Taxol. *Cancer Res* 2003; **63**:2139–2144.
28 Bagatell R, Khan O, Paine-Marrieta G, Taylor CW, Akinaga S, Whitesell L. Destabilization of steroid receptors by heat shock protein 90-binding drugs: a ligand-independent approach to hormonal therapy of breast cancer. *Clin Cancer Res* 2001; **7**:2076–2084.
29 Kamal A, Thao L, Sensintaffar J, Zhang L, Boehm MF, Fritz LC, *et al.* A high-affinity conformation of Hsp90 confers tumour selectivity on Hsp90 inhibitors. *Nature* 2003; **425**:407–410.

30 Banjeri U, O'Donnell A, Scurr M, Benson C, Hanwell J, Clark S, *et al.* Phase I trial of the heat shock protein 90 (Hsp90) inhibitor 17-allylamino-17-demethoxygeldanamycin (17aag). Pharmacokinetic (PK) profile and pharmacodynamic (PD) endpoints. *Proc Am Soc Clin Oncol* 2001; **20**:82a.
31 Wilson RH, Takimoto CH, Agnew EB, Morrison G, Grollman F, Thomas RR, *et al.* Phase I pharmacological study of 17-(allylamino)-17-demethoxygeldanamycin (AAG) in adult patients with advanced solid tumors. *Proc Am Soc Clin Oncol* 2001; **20**:82a.
32 Münster PN, Tong W, Schwartz L, Larson S, Keneson K, De La Cruz A, *et al.* Phase I trial of 17-(allylamino)-17-demethoxygeldanamycin (17-AAG) in patients (pts) with advanced solid malignancies. *Proc Am Soc Clin Oncol* 2001; **20**:83a.
33 Banerji U, Clake P, Walton M, O'Donnel A, Raynaud F, Turner A, *et al.* Preclinical an clinical activity of the molecular chaperone inhibitor 17-allylamino, 17-demethoxygeldanamycin(17AAG) in malignant melanoma. *Proc Am Ass Cancer Res* 2003; **44**:677 (abstr 2966).